A&A 487, 363–367 (2008)
DOI: 10.1051/0004-6361:20079236

Astronomy & Astrophysics

Collisional activation of asteroids in cometary orbits[⋆]

C. G. Díaz[2] and R. Gil-Hutton[1,2]

[1] Complejo Astronómico El Leoncito – CONICET – Av. España 1512 sur, J5402DSP San Juan, Argentina
e-mail: `rgilhutton@casleo.gov.ar`
[2] Universidad Nacional de San Juan – Av. J. I. de la Roza 590 oeste, 5400 Rivadavia, San Juan, Argentina
e-mail: `siempregonza@hotmail.com`

Received 12 December 2007 / Accepted 27 April 2008

ABSTRACT

Aims. We study the time an asteroid in a cometary orbit must wait to receive a collision producing a crater depth enough to expose subsurface volatiles, aiming to analyze the possibility of collisional reactivation of these objects if they are dormant comets.
Methods. We perform a numerical integration of the asteroids in cometary orbits and a population of projectiles to find the mean intrinsic collision probabilities and mean impact velocities of the targets. The projectile population was obtained as a sample with the same distribution of orbital elements as observed for main belt asteroids, and we also take into account that its size distribution changes for different size ranges. Only 206 asteroids in cometary orbits, that are not members of other asteroid groups, with a Tisserand parameter $2 \leq T_J \leq 2.9$ and perihelion distance $q > 1.3$ AU were considered.
Results. A large fraction of the objects in the sample receive at least 1 collision energetic enough to break the comet crust and allow a dormant comet to reach an active state in a period shorter than a Jupiter Family Comet dynamical lifetime. A large fraction of the objects in the sample with $r_t \geq 8$–9 km receive several collisions and could be active for more than 3×10^4 yr. We found an excess in the number of dormant comet candidates from the expected values which is indicative of the presence in the ACOs population of objects that are not comets in a dormant state. These objects could be asteroids with $T_J < 3$ that reach their present orbits by some dynamical mechanism that perturbs the original asteroidal orbit changing its Tisserand invariant.

Key words. minor planets, asteroids – comets: general – solar system: general

1. Introduction

The different formation regions of asteroids and comets in the Solar System produced differences in their physical properties. Asteroids are planetesimals formed during the early ages of the Solar System in the region between Mars and Jupiter while comets were formed in a region that extends from the giant planets to the outer limits of the pre-solar nebula. As a consequence, there is a significant difference in the content of volatile material in both populations. This fact has provided the most apparent distinction between members of these two populations: comet nuclei, when close to the Sun, are usually surrounded by a coma produced by the out-gassing of volatiles caused by solar heating, while asteroids are not. This simple distinction has some complications due to the discovery of icy objects that rarely develop a coma due to their distance from the Sun, the discovery of asteroids with dynamical properties similar to those of comets, and the discovery of objects in typical asteroidal orbits that show temporary comet-like activity.

At the end of their active life some comets might develop an asteroidal appearance when sublimation stops and reaches dormancy or extinction due to the depletion of volatile material or by a crust built up on their surfaces (Rickman et al. 1990; Kührt & Keller 1994; Benkhoff & Huebner 1996; Jewitt 2002). The gas activity of a cometary nucleus coming close to the Sun can form a layer of dust grains that are too heavy to be blown off by the gas outflow. This crust could eventually become so thick that subsurface volatiles cannot be warmed up to sublimation temperature, ceasing any cometary activity, and the nucleus appears observationally identical to an asteroid. Since this crust does not completely stop the vapor production in the comet interior, it could be possible that a large amount of ice is present below it even though the comet reaches an inactive state (Prialnik & Mekler 1991).

One way to reactivate dormant comets is by means of impacts with interplanetary bodies. Fernández (1990) and Matese & Whitman (1994) tried to explain the outburst activity of comets by impacts with small asteroids or meteoroids, and some authors have the opinion that this is the case for comets 41P/Tuttle-Giacobini-Kresák (Kresák 1974; Fernández 1981), 72P/Denning-Fujikawara (Beech 2001), and 133P/Elst-Pizarro (Toth 2000), while Toth (2001) suggested that the splitting of the comet C/1994 S4 (LINEAR) was a result of a collision of the comet with asteroid debris. Collisions of interplanetary boulders with a dormant comet could result in craters that partially destroy the crust on its surface, triggering reactivation by allowing the fresh material buried below the crust to begin sublimation in the next perihelion passage.

The dynamical criterion used to define the sample of objects that are candidate dormant comets is related to the Tisserand parameter (Kresák 1979), which is defined by the relation $T_J = a_J/a + 2\cos I\sqrt{(a/a_J)(1-e^2)}$, where a and a_J are the semimajor axis of the orbits of the object and Jupiter, respectively, while e and I are the eccentricity and inclination relative to the orbital plane of Jupiter of the object's orbit. By this criterion, cometary orbits are defined as those having $T_J < 3$, while asteroidal orbits are those with $T_J > 3$. Therefore, all the objects with $T_J < 3$ that do not present any signature of cometary activity are defined as

---

[⋆] Table 1 is only available in electronic form at
`http://www.aanda.org`

an asteroid in a cometary orbit (ACO). Objects with $T_J < 2$ have been called Damocloids by Jewitt (2005) and are asteroids in Halley-type cometary orbits, while those with $2 \leq T_J \leq 3$ have orbits similar to the Jupiter family comets (JFCs). Therefore, ACOs are good candidates to be extinct or dormant comets.

Licandro et al. (2005) found differences in the spectroscopic properties of two sub-samples of ACOs, the near Earth objects (NEOs) with perihelion distance $q \leq 1.3$ AU and the non-NEOs, these last objects being spectroscopically similar to cometary nuclei. These authors also found that ACOs with featured spectra typical of the main belt have $T_J \geq 2.9$ while those with $T_J < 2.9$ shown comet-like spectra, suggesting that the sub-sample of ACOs with $2.9 \leq T_J \leq 3.0$ could be contaminated by a large fraction of interlopers from the inner part of the belt. On the other hand, Alvarez-Candal & Licandro (2006) found that the sub-sample of ACOs with $q > 1.3$ AU has a size distribution similar to that of the Jupiter family comets and can be composed of a significant fraction of dormant comets, while a large fraction of ACOs with $q < 1.3$ AU could be scattered objects from the outer main belt.

The purpose of this paper is to analyze the possibility of reactivation of dormant comets by collisions with interplanetary boulders. Since the physical properties of JFCs are better known than for other comets and taking into account the above considerations, we only consider as dormant comet candidates ACOs with $2 \leq T_J \leq 2.9$ and $q > 1.3$ AU. In Sect. 2 we describe the computational method used and in Sects. 3 and 4 we present and discuss our results. In Sect. 5 we present our conclusions.

2. Computational method

In order to break the cometary crust and allow the dormant comet to reactivate in the next perihelion passage, it is necessary to break the target surface with impact craters deep enough to reach the buried ice. The crater diameter D_c produced by a collision with a projectile of radius r_p and impact velocity v_p is found using the expression proposed by Zahnle et al. (1998):

$$D_c = 1.70 r_p^{0.78} g^{-0.22} v_p^{0.44} \left(\frac{\rho_p}{\rho_t}\right)^{0.333} (\cos\theta)^{0.44}, \quad (1)$$

which is essentially the expression recommended by Schmidt & Housen (1987) but considering that only the normal component of the impact velocity contributes to cratering. In this equation ρ_t and ρ_p are the densities for the comet and projectile, respectively, g is the surface gravity on the comet, θ is the incidence angle measured from the zenith, and the equation must be evaluated in cgs units. The mean value of θ for the normal component of isotropic velocities is 45° and we always assume densities of $\rho_t = 0.5$ g cm^{-3} and $\rho_p = 2.5$ g cm^{-3} for ACOs and projectiles, respectively. The exposed area produced by the crater is:

$$A_c = \pi \left(\frac{D_c^2}{4} + h_c^2\right), \quad (2)$$

where h_c is the crater depth. If the crust thickness is h, to reach the ice below the crust we need $h_c \geq h$ and using the crater depth/diameter ratio, which is almost constant for simple craters and equal to 0.18–0.20 for the Moon and icy Galilean satellites (Schenk et al. 2004), it is possible to find the radius r_p of the projectile needed to form such crater.

On the other hand, the mean number of impacts received by the comet with projectiles of radius larger than r_p in a time Δt is:

$$\begin{aligned} \langle N_{\rm col}(> r_p)\rangle &= \langle P_i\rangle (r_t + r_p)^2 \Delta t N_{\rm pro}(> r_p) \\ &\approx \langle P_i\rangle r_t^2 \Delta t N_{\rm pro}(> r_p), \end{aligned} \quad (3)$$

where r_t is the comet radius, $\langle P_i\rangle$ is the mean intrinsic collision probability between the comet and the projectile population, $N_{\rm pro}(> r_p)$ is the number of projectiles in the population with radius larger than r_p, and $r_p \ll r_t$. The comet radius has been computed from the absolute magnitude of the object, H, by:

$$\log(p_v \pi r_t^2) = 16.85 + 0.4(m_\odot - H), \quad (4)$$

where the result is in kilometers, $m_\odot = -26.77$ is the apparent visual magnitude of the Sun, and a standard albedo $p_v = 0.04$ was assumed.

Mean intrinsic collision probabilities and mean impact velocities can be inferred from statistical studies of the occurrence of orbital encounters between the comet and the projectile population, so we decided to estimate these parameters using the numerical method developed by Marzari et al. (1996). In this method the target and a projectile population were numerically integrated over a time span $T_{\rm int}$ and the encounter distance and encounter velocity between the target and any projectile were recorded. Since Marzari et al. showed that the distribution of the cumulative number of encounters for an encounter distance less than $d_{\rm enc}$ is proportional to $d_{\rm enc}^2$, a distribution of the form:

$$N_{\rm enc}(< d_{\rm enc}) = P_1 \times d_{\rm enc}^2 \quad (5)$$

was assumed. P_1 is found by a fit to the data, taken as the standard deviation for each point $\sqrt{N_{\rm enc}}$. Then, the mean intrinsic collision probability is obtained from:

$$\langle P_i\rangle = \frac{P_1}{n_{\rm pair} T_{\rm int}}, \quad (6)$$

where $n_{\rm pair}$ is the number of different pairs of objects that can be formed within the interacting population.

Since the asteroid belt is the main source of projectiles, it is enough to use as the interacting population a sample of particles with the same orbital element distribution as that observed for the objects in the asteroid belt. This sample was obtained as follows: first, the objects that form the complete known asteroid population, i.e., those asteroids with mean apparent opposition V magnitudes $V(a, 0) < 15.75$ (Tedesco et al. 2005), and with semimajor axis $a > 2$ AU were taken from the ASTORB database (`ftp://ftp.lowell.edu/pub/elgb/astorb.html`) to get a first sample of 4549 objects. Then, a six-dimensional distribution of the orbital elements was calculated and a final sample of 350 particles was obtained at random from it. The hybrid integrator EVORB (Fernández et al. 2002) was used for the numerical integration of the targets and the particles of the interacting population, under the gravitational influence of the Sun and the planets from Mercury to Neptune. The integration was performed over a time span of $T_{\rm int} = 10^5$ yr, and a encounter was recorded every time the mutual distance between the target and a particle was less than 0.05 AU.

To find a value for $N_{\rm pro}(> r_p)$ it is necessary to know the cumulative size distribution of the real projectile population, i.e. the size distribution of the main asteroid belt. We assume an exponential size distribution of the form $dN_{\rm pro}(> r) \propto r^{-b} dr$, where b is a characteristic exponent. Taking into account that the main belt size distribution changes for different size ranges, we have:

$$\begin{aligned} N_{\rm pro}(> r_p) &= N_{\rm pro}(> 500\ {\rm m}) \\ &\quad + K_0 \int_{r_c}^{500\ {\rm m}} r^{-b_0} dr + K_1 \int_{r_p}^{r_c} r^{-b_1} dr, \end{aligned} \quad (7)$$

where $N_{\mathrm{pro}}(> 500\ \mathrm{m}) = 1.36 \times 10^6$ is the number of objects in the asteroid belt with radius larger than 500 m (Farinella & Davis 1992; Tedesco & Desert 2002; Morbidelli & Vokrouhlický 2003; Bottke et al. 2005). The size distribution of very small main belt asteroids is not well known, so it is not easy to choose values for the parameters r_c, K_0, b_0, K_1, and b_1. We decide to use two size distributions with $r_c = 200$ m and 100 m, respectively, and to assume the size distribution proposed by Yoshida & Nakamura (2007) in the size range $r_c < r < 500$ m ($b_0 = 2.29$), and a Dohnanyi (1969) size distribution for objects smaller than r_c ($b_1 = 3.5$). Using this combined size distribution the total number of objects with a radius larger than 0.5 m is 1.42×10^{13} in the first case and 6.11×10^{12} in the second.

3. Results

The minimum ice exposed area needed to consider the comet as active could be obtained from the known JFC population. Almost all the studied JFCs have a fraction of active surface area below ~10–20%, with a large fraction of active area for the smaller comets and a very small one for the few observed comets with $r_t > 3$ km (Tancredi et al. 2006). This could be indicative of a condition of the minimum effective exposed area to consider a comet as active, which could be proportional to r_t^{-2}. Thus, we assume that a comet could reach an active state during the next perihelion passage when its exposed area is at least 10% of the total surface area of an object with radius 1 km (1.257 km^2). With this definition an object must have a radius larger than 0.316 km to have the possibility of being active, because for smaller objects its total surface area is always less than the required exposed one.

There are different values for the mantle thickness in the literature, ranging from a few millimeters to several centimeters. Since we must be sure that the crater excavates the surface enough to reach the ice below it, only craters with a minimum depth of $h = 1$ m are considered to calculate the exposed area.

A sample of 206 dormant comets candidates was obtained from the ASTORB database, considering only ACOs with $2 \leq T_J \leq 2.9$ and $q > 1.3$ AU, and excluding objects with 3.03 AU $< a <$ 3.70 AU, $e < 0.4$ and $i < 25°$ (possibly main belt or Cybele asteroids), with 3.70 AU $< a <$ 4.20 AU, $e < 0.4$ and $i < 20°$ (Hildas), and with 5.00 AU $< a <$ 5.40 AU, and $e < 0.3$ (Trojans). The absolute magnitude and radius of the ACO, mean intrinsic collisional probability, mean collision velocity and its error, the radius of the projectile that produces a crater with the minimum exposed area, and the times needed to receive such a collision for the two projectile size distributions ($r_c = 200$ m and 100 m, respectively) are listed in Table 1. The errors of the mean intrinsic collision probabilities are always less than 10^{-22} km^{-2} yr^{-1} for all the objects. Twenty seven ACOs (5164, 30512, 32511, 37117, 96177, 1983JZ_1, 1995 WL_3, 2000 AU$_{242}$, 2000 QD$_{181}$, 2000 WT_{168}, 2000 XO_8, 2001 QG_{288}, 2003 BM_1, 2003 UR_{267}, 2004 BT_1, 2004 KZ_7, 2004 RW_{141}, 2005 EB_{127}, 2005 JE_{173}, 2005 NX_{43}, 2005 XK_{57}, 2005; YW_{24}, 2006 BV_7, 2006 HS, 2006 HP_{131}, 2006 JO_{65}, and 2006 SO_{134}) had one or more close encounters with the planets and escaped before the integration ended. Then, their mean intrinsic collisional probability and mean collision velocity were calculated over a shorter time span, as indicated in Table 1.

4. Discussion

If the ACOs in our sample are dormant comets from the Jupiter family, their dynamics are also dominated by close encounters with this planet producing strong perturbations in their orbits. Fernández et al. (2002) found that the dynamical lifetime of Jupiter family comets is ~2×10^5 yr, which are relatively short compared to other populations. Assuming that this dynamical lifetime is also valid for the ACOs in our sample, the results presented here show that 53% and 32% of the objects in the sample receive at least 1 collision energetic enough to break the comet crust and allow a dormant comet to reach an active state in a period shorter than a JFC dynamical lifetime, 37% and 16% receive 2 or more collisions, 26% and 11% receive at least 3, and 16% and 7% receive not fewer than 4, for projectile distributions with $r_c = 200$ m and 100 m, respectively (Fig. 1). Then, many objects in the ACOs sample received 1 or more collisions during their dynamical lifetimes and, if they are dormant comets, they could be reactivated.

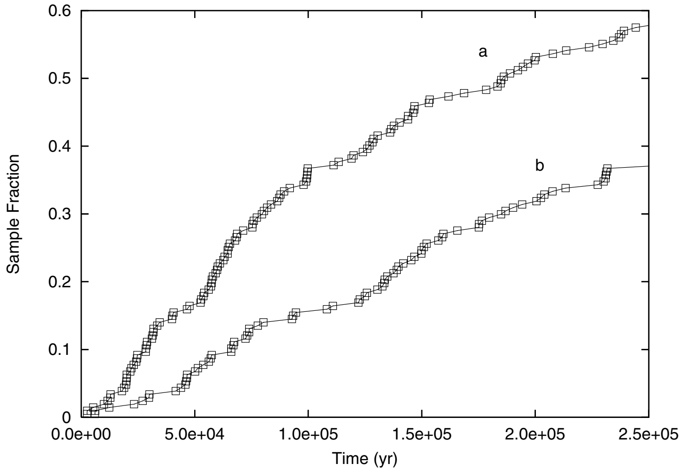

Fig. 1. Fraction of ACO sample reaching the minimum exposed area to be considered as active comets in a certain time, for a projectile size distribution with **a)** $r_c = 200$ m, and **b)** $r_c = 100$ m. Only times shorter than the dynamical lifetime of Jupiter family comets are considered.

On the other hand, in spite of their short dynamical lifetimes, comets become inactive mainly by physical causes due to a steady mass loss by sublimation of volatiles or by formation of a dust mantle. Based on the mean rate of secular brightness decrease, Kresák & Kresáková (1990) have estimated a mean active lifetime of ~6×10^3 yr for JFCs with a perihelion distance less than 1.5 AU, while Fernández (1985) found a lifetime of ~2×10^4 yr for these objects. Taking 1×10^4 yr as a working value for the mean active lifetime of JFCs before they become dormant, and assuming that each time a dormant comet receives a collision energetic enough to expose fresh ices it becomes active for at least half the initial active period (5×10^3 yr), it is expected to see these objects in an active state during a significant fraction of their dynamical lifetimes. As shown in Fig. 2 and Table 1, a large fraction of the largest objects in the ACO sample ($r_t \geq 8$–9 km) receives more than 4 collisions during this period and could be active during more than 3×10^4 yr.

Using this result we can compare the present number of objects in the active comet and ACO sample to test our initial assumption that they are dormant comets. Since the population of dormant comet candidates must be seriously affected by an observational bias, which is more serious for the smaller and fainter objects, to allow a direct comparison only the largest objects in both populations are taken into account to minimize the bias effect. Then, using the radii of JFCs obtained by Tancredi et al. (2006), we found for the active population only 1 comet with

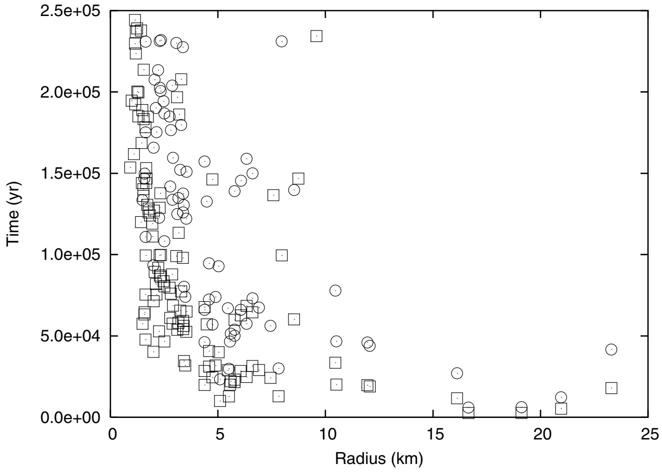

Fig. 2. Time needed to receive a collision energetic enough to reactivate a dormant comet in function of its radius. Only objects with collision time shorter than 2.5×10^5 yr are shown. The results for the projectile distributions with r_c = 200 m and 100 m are indicated with squares and circles, respectively.

radius larger than 9 km, 2 objects with radius larger than 5 km, and 5 objects with radius larger than 4 km. Taking into account these values and the period the comets are in an active state found previously, we must expect ~6, ~12 and ~32 dormant comets in each radius range, respectively. In the ACO sample we found 15, 46 and 59 objects, respectively, that are in excess from the expected values and are indicative of the presence in the ACO population of objects that are not comets in a dormant state. These objects could be asteroids (possibly Hildas) with $T_J < 3$ obtaining their present orbits by some dynamical mechanism that perturbed the original asteroidal orbit changing its Tisserand invariant (Di Sisto et al. 2005).

The objects (1373) Cincinatti, (2938) Hopi, and (20898) Fountainhills receive collisions energetic enough to reactivate a dormant comet at a rate of >1–2×10^{-4} yr^{-1}, depending on the projectile size distribution. With these collision rates, they are the best candidates in the ACO sample to be observed during a reactivation if they are dormant comets.

While all the assumptions made here are reasonable, it is necessary to consider two of them more deeply. First, if the projectile size distribution used for the calculations is not accurate, the results presented here could be highly modified. Since the size distribution changes for different size ranges and for very small objects is not well known, it is not easy to choose values for their parameters in the smaller size end of the distribution. As a first guess we used the size distribution proposed by Yoshida & Nakamura (2007) for objects with a radius between 500 m and 200 or 100 m, in spite that these authors proposed it for objects larger than 250 m. It is possible that this size distribution could be still valid for smaller objects (for example, for $r \lesssim 100$ m) producing a shallow size distribution and a shortage of small projectiles, making the ACO collisional reactivation process very improbable. Nevertheless, this shallow size distribution extended to very small sizes is difficult to reconcile with the cratering records of (243) Ida, (253) Mathilde, and (951) Gaspra (Chapman 2002).

Second, the choice of the minimum exposed area on the cometary surface to be considered active during its next perihelion passage is rather arbitrary. Taking the double of the original value (20% of the total surface area of an object with radius 1 km), the radius of the projectile needed to make a crater with that dimension is 1.56 times the original radius and the time needed to receive such a collision is 2–3 times longer, depending on the size distribution used and if the radius of the projectile is larger or smaller than r_c. In this case, 37% and 16% of the objects in the sample receive at least 1 collision energetic enough to break the comet crust and allow a reactivation, and 16% and 7% receive more than 2 collisions for the projectile distributions with r_c = 200 m and 100 m, respectively. Then, the objects in the ACO sample with $r_t \geq 8$–9 km receive more than 2 collisions during this period and could be active during >10% of their dynamical lifetimes, and we must expect ~9, ~18 and ~45 dormant comets for a comet radius of >9 km, >5 km, and >4 km, respectively, which are also indicative of the presence in the ACO population of objects that are not comets in a dormant state.

5. Conclusions

We compute the mean intrinsic collision probability, the mean collision velocity, and the time needed to be reactivated by a collision for a sample of 206 ACOs that are dormant comet candidates from the Jupiter family.

The results presented here show that a large fraction of the objects in the sample receive at least 1 collision energetic enough to break the comet crust and allow a dormant comet to reach an active state in a period shorter than a JFC dynamical lifetime. A large fraction of the objects in the ACO sample with $r_t \geq 8$–9 km receive several collisions and could be active during more than 3×10^4 yr.

Three objects, (1373) Cincinatti, (2938) Hopi, and (20898) Fountainhills, receive collisions energetic enough to reactivate a dormant comet at a high rate, being the best candidates in the ACO sample of being observed during a reactivation if they are dormant comets.

Comparing only the largest objects in the active JFC population and ACO sample, we found an excess in the number of dormant comet candidates from the expected values which is indicative of the presence in the ACO population of objects that are not comets in a dormant state. These objects could be asteroids with $T_J < 3$ obtaining their present orbits by a dynamical mechanism that perturbs the original asteroidal orbit, changing its Tisserand invariant.

Acknowledgements. The authors wish to thanks J. A. Fernández for his comments and suggestions. The authors acknowledge the partial financial support by CICITCA, Universidad Nacional de San Juan, through a research grant.

References

Alvarez-Candal, A., & Licandro, J. 2006, A&A, 458, 1007
Beech, M. 2001, MNRAS, 327, 1201
Benkhoff, J., & Huebner, W. F. 1996, Planet. Space Sci., 44, 1005
Bottke, W. F., Durda, D. D., Nesvorný, et al. 2005, Icarus, 179, 63
Chapman, C. R. 2002, in Asteroids III, ed. W. F. Bootke, Jr., A. Cellino, P. Paolicchi, & R. P. Binzel (Tucson: Univ. of Arizona Press), 315
Di Sisto, R. P., Brunini, A., Dirani, L., & Orellana, R. B. 2005, Icarus, 174, 81
Dohnanyi, J. W. 1969, J. Geophys. Res., 74, 2531
Farinella, P., & Davis, D. R. 1992, Icarus, 97, 111
Fernández, J. A. 1981, Moon Plan., 25, 507
Fernández, J. A. 1985, Icarus, 64,308
Fernández, J. A. 1990, in Asteroids, Comets, Meteors III, ed. C.-I. Lagerkvist, H. Rickman, B. A. Lindblad, & M. Lindgren, Uppsala University, Uppsala, 309
Fernández, J. A., Gallardo, T., & Brunini, A. 2002, Icarus, 159, 358
Jewitt, D. 2002, AJ, 123, 1039
Jewitt, D. 2005, AJ, 129, 530

Kresák, L. 1974, Bull. Astron. Inst. Czechosl., 25, 293
Kresák, L. 1979, in Asteroids, ed. T. Gehrels (Tucson: Univ. of Arizona Press), 289
Kresák, L., & Kresáková, M. 1990, Icarus, 86, 82
Kührt, E., & Keller, H. U. 1994, Icarus, 109, 121
Licandro, J., de León, J., Pinilla, N., & Serra-Ricart, M. 2005, Adv. Space Res., 38, 1991
Marzari, F., Scholl, H., & Farinella, P. 1996, Icarus, 119, 192
Matese, J. J., & Whitman, P. G. 1994, Icarus, 109, 258
Morbidelli, A., & Vokrouhlický, D. 2003, Icarus, 163, 120
Prialnik, D., & Mekler, Y. 1991, ApJ, 366, 318
Rickman, H., Fernández, J. A., & Gustafson, B. 1990, A&A, 237, 524
Schenk, P. M., Chapman, C., Moore, J., & Zahnle, K. 2004, in Jupiter: Planet, Satellites, and Magnetosphere, ed. F. Bagenal, & W. McKinnon (Cambridge: Cambridge Univ. Press), 427
Schmidt, R. M., & Housen, K. R. 1987, Int. J. Impact Eng., 5, 543
Tancredi, G., Fernández, J. A., Rickman, H., & Licandro, J. 2006, Icarus, 182, 527
Tedesco, E. F., & Desert, F. 2002, AJ, 123, 2070
Tedesco, E. F., Cellino, A., & Zappalá, V. 2005, AJ, 129, 2869
Toth, I. 2000, A&A, 360, 375
Toth, I. 2001, A&A, 368, L25
Yoshida, F., & Nakamura, T. 2007, Planet. Space Sci., 55, 1113
Zahnle, K., Dones, L., & Levison, H. F. 1998, Icarus, 136, 202

Table 1. Physical and collisional parameters for ACOs in the dormant comet candidate sample.

	ACO	H	r_t km	$\langle P_i \rangle$ km^{-2} yr^{-1}	$\langle V_{col} \rangle$ km s^{-1}	$\sigma_{v_{col}}$ km s^{-1}	r_a m	T_{200} yr	T_{100} yr
(944)	Hidalgo	10.77	23.30	0.16E-18	17.90	2.80	172.09	17 930	41 636
(1373)	Cincinnati	11.20	19.12	0.21E-17	13.21	2.55	193.16	2669	6198
(1922)	Zulu	12.20	12.06	0.52E-18	13.68	2.89	166.32	18 913	43 919
(2938)	Hopi	11.50	16.65	0.24E-17	13.92	2.63	180.37	2595	6026
(5164)	Mullo[1]	13.10	7.97	0.21E-18	11.85	2.88	160.46	99 502	231 065
(6144)	1994 EQ3	11.50	16.65	0.59E-19	7.18	2.25	262.04	272 545	632 909
(7604)	Kridsadaporn	13.70	6.05	0.99E-18	12.17	2.78	146.21	28 453	66 075
(8373)	Stephengould	13.80	5.77	0.11E-17	14.58	2.96	130.34	21 606	50 174
(9767)	Midsomer Norton	16.40	1.74	0.45E-18	17.74	4.09	83.24	184 721	428 964
(17493)	Wildcat	14.30	4.59	0.99E-18	14.72	3.26	121.49	31 159	72 357
(18916)	2000 OG44	14.30	4.59	0.22E-18	8.94	3.31	160.95	286 006	664 170
(20898)	Fountainhills	11.00	20.96	0.73E-18	15.78	2.66	179.33	5326	12 367
(30512)	2001 HO8 [2]	12.50	10.51	0.98E-18	9.42	2.58	197.44	20 093	46 662
(32511)	2001 NX17 [3]	12.70	9.58	0.12E-18	8.21	2.66	207.89	234 349	544 210
(37117)	2000 VU2 [4]	13.20	7.61	0.18E-19	7.00	1.90	213.15	2 488 569	5 779 010
(37384)	2001 WU1	14.30	4.59	0.94E-18	12.67	2.83	132.21	40 718	94 557
(41461)	2000 ON	13.90	5.51	0.19E-17	14.73	2.92	127.92	12 859	29 861
(88043)	2000 UE110	14.40	4.38	0.14E-17	16.11	3.23	113.97	19 897	46 204
(96177)	1984 BC [5]	16.20	1.91	0.15E-18	12.38	3.16	104.66	827784	1 922 300
(101795)	1999 HX2	15.30	2.89	0.13E-17	12.13	2.75	119.00	57 568	133 687
(115916)	2003 WB8	14.10	5.03	0.87E-18	12.41	2.69	137.29	39 967	92 812
(116908)	2004 GT2	14.90	3.48	0.20E-17	11.47	2.40	129.36	31 869	74 006
(136620)	1994 JC	15.10	3.17	0.33E-18	18.09	4.20	97.48	11 3411	263 365
(138512)	2000 LE3	13.60	6.33	0.10E-17	12.72	2.90	144.48	24 769	57 519
(144870)	2004 MA8	14.40	4.38	0.17E-17	11.16	2.53	140.19	28 460	66 091
(145485)	2005 UN398	13.80	5.77	0.65E-18	10.10	3.36	160.33	59 856	139 000
(145627)	2006 RY102	11.10	20.02	0.12E-20	5.46	1.44	322.12	15 9755 62	37 098 808
	1983 JZ1 [6]	13.60	6.33	0.36E-18	12.74	2.88	144.35	68 440	158 932
	1989 FR	11.57	16.12	0.79E-18	10.91	2.63	205.08	11 669	27 099
	1992 XA	17.35	1.13	0.92E-19	9.71	2.94	103.37	3 710 281	8 616 097
	1995 KG1	19.39	0.44	0.87E-18	16.22	4.29	59.38	644 006	1 495 526
	1995 WL3 [7]	19.01	0.52	0.43E-18	11.93	3.27	74.19	1 612 762	3 745 191
	1997 GF3	17.43	1.08	0.74E-18	14.11	3.13	82.86	285 659	663 363
	1997 UR14	16.84	1.42	0.17E-17	11.36	2.65	101.10	119 978	278 617
	1998 BC34	20.84	0.23	0.20E-17	11.43	2.83	59.92	1 098 889	2 551 865
	1998 HO121	12.27	11.68	0.17E-19	8.07	1.68	221.97	1 247 648	2 897 316
	1998 KK56	16.35	1.78	0.11E-17	12.22	2.71	103.39	125 975	292 542
	1998 QJ1	16.73	1.50	0.11E-18	13.96	2.48	91.29	1 245 167	2 891 554
	1998 UQ1	16.55	1.63	0.62E-18	15.46	3.97	88.23	178 360	414 192
	1998 WL34	14.16	4.89	0.65E-20	5.64	1.04	212.55	16 852 414	39 135 052
	1999 TM113	13.92	5.46	0.11E-17	12.56	2.45	139.59	28 856	67 010
	1999 XB69	16.41	1.74	0.66E-19	10.84	2.57	109.77	2 536 811	5 891 039
	1999 XD106	16.48	1.68	0.97E-18	12.50	2.92	100.37	146 770	340 833
	1999 XO188	13.51	6.60	0.84E-18	11.76	3.49	152.79	31 481	73 106
	2000 AC229	16.65	1.55	0.42E-18	18.59	3.78	78.49	213 616	496 063

[1] T_{int} = 77 563 yr.
[2] T_{int} = 18 033 yr.
[3] T_{int} = 75 521 yr.
[4] T_{int} = 54 421 yr.
[5] T_{int} = 86 800 yr.
[6] T_{int} = 50 501 yr.
[7] T_{int} = 86 502 yr.

Table 1. continued.

ACO	H	r_t km	$\langle P_i \rangle$ km^{-2} yr^{-1}	$\langle V_{col} \rangle$ km s^{-1}	$\sigma_{v_{col}}$ km s^{-1}	r_a m	T_{200} yr	T_{100} yr
2000 AU242 [8]	13.41	6.91	0.99E-18	10.66	3.86	163.61	29 015	67 380
2000 BK2	16.72	1.50	0.41E-19	10.03	2.60	110.16	5 406 868	12 555 950
2000 CA13	17.90	0.87	0.49E-18	11.54	3.09	87.31	759 727	1 764 254
2000 EJ37	13.21	7.58	0.12E-18	14.69	3.15	140.13	136 520	317 029
2000 GQ132	17.24	1.18	0.89E-18	13.08	2.88	88.64	236 828	549 967
2000 GH147	17.62	0.99	0.12E-17	14.54	3.37	79.48	19 4581	45 1861
2000 KD41	16.60	1.59	0.25E-17	12.03	2.69	100.98	64 513	149 813
2000 OZ21	16.33	1.80	0.83E-19	11.01	3.55	109.94	1 883 303	4 373 448
2000 QJ46	15.37	2.80	0.22E-19	8.67	2.08	142.51	5 619 233	13 049 109
2000 QD181 [9]	15.08	3.20	0.60E-18	8.23	2.57	152.40	186 129	432 234
2000 SB1	15.02	3.29	0.71E-18	13.28	2.81	117.26	77 370	179 670
2000 SL44	15.61	2.51	0.18E-17	12.85	2.92	110.64	46 601	108 218
2000 SO182	13.69	6.07	0.80E-18	8.04	2.30	184.97	62 612	145 399
2000 TG24	15.81	2.29	0.63E-18	13.97	3.27	102.84	128 804	299 112
2000 WT168 [10]	14.35	4.48	0.67E-18	12.90	3.55	130.03	57 129	132 666
2000 XO8 [11]	15.54	2.59	0.18E-18	10.61	2.92	124.39	564 616	1 311 164
2000 YN30	16.82	1.44	0.19E-18	13.02	3.01	93.85	856 170	1 988 216
2000 YL90	13.87	5.59	0.15E-17	11.73	2.62	146.02	22 141	51 416
2001 CT20	15.29	2.91	0.10E-17	12.47	2.80	117.31	68 690	159 514
2001 HW18	17.64	0.98	0.66E-18	15.16	4.17	77.43	329 400	764 941
2001 HJ30	17.04	1.30	0.11E-17	11.99	2.86	95.55	184 993	429 595
2001 JO	14.96	3.38	0.11E-17	12.38	2.82	122.95	54 194	125 851
2001 KX67	16.16	1.95	0.10E-17	12.44	2.86	104.92	119 059	276 481
2001 OK17	18.71	0.60	0.11E-17	16.06	3.08	65.23	345 238	801 719
2001 QF6	14.97	3.37	0.50E-18	14.05	3.25	114.33	97 966	227 498
2001 QS145	16.62	1.58	0.24E-17	12.82	2.66	97.17	63 192	146 746
2001 QQ199	12.22	11.95	0.53E-18	13.17	3.12	169.48	19 780	45 933
2001 QG288 [12]	15.69	2.42	0.40E-18	8.41	2.59	139.08	390 587	907 030
2001 SK276	17.31	1.15	0.95E-18	11.56	3.16	94.18	273 585	635 326
2001 TX16	13.90	5.51	0.13E-18	10.95	3.54	151.21	287 255	667 069
2001 UO16	17.53	1.04	0.14E-17	9.99	2.70	99.38	263 461	611 816
2001 VE	15.05	3.25	0.12E-17	10.19	2.69	135.62	65 515	152 140
2001 WX1	14.95	3.40	0.11E-17	11.63	2.82	127.52	56 175	130 452
2001 XN88	18.62	0.63	0.12E-17	14.47	3.29	69.99	358 418	832 327
2001 XW150	16.78	1.46	0.48E-18	9.46	3.48	112.97	530 463	1 231 854
2001 YK61	13.76	5.88	0.20E-20	8.57	2.62	176.82	23 498 712	54 569 236
2002 AA16	15.80	2.30	0.11E-17	12.16	2.68	111.36	87 189	202 471
2002 AW33	16.93	1.37	0.67E-18	10.84	2.93	102.60	339 665	788 777
2002 AO148	12.67	9.71	0.56E-19	6.78	1.91	232.49	627 359	1 456 867
2002 JC68	16.50	1.66	0.91E-18	12.80	2.97	98.78	153 139	355 623
2002 JE109	18.57	0.64	0.19E-17	9.96	2.88	86.97	366 299	850 627
2002 JW115	15.81	2.29	0.59E-18	17.59	3.54	90.31	99 617	231 334
2002 KJ8	20.25	0.30	0.27E-17	10.10	2.73	69.37	667 800	1 550 781
2002 LJ27	18.01	0.83	0.87E-18	11.87	3.17	84.72	437 563	1 016 120
2002 MO3	16.55	1.63	0.17E-17	18.96	3.01	78.63	47 734	110 849
2002 OL15	18.27	0.74	0.18E-17	8.24	3.12	100.63	415 792	965 562
2002 PA96	15.14	3.11	0.13E-17	12.02	2.82	122.12	53 806	124 950
2002 QC25	17.14	1.24	0.81E-18	13.32	2.91	88.88	239 026	555 071

[8] $T_{int} = 8142$ yr.

[9] $T_{int} = 61\,536$ yr.

[10] $T_{int} = 83\,083$ yr.

[11] $T_{int} = 69\,831$ yr.

[12] $T_{int} = 52\,223$ yr.

Table 1. continued.

ACO	H	$r_{\rm t}$ km	$\langle P_{\rm i}\rangle$ km^{-2} yr^{-1}	$\langle V_{\rm col}\rangle$ km s^{-1}	$\sigma_{v_{\rm col}}$ km s^{-1}	r_a m	T_{200} yr	T_{100} yr
2002 RQ28	18.44	0.68	0.15E-18	8.92	3.29	94.13	5 080 341	11 797 681
2002 SU	16.74	1.49	0.18E-17	17.24	2.90	80.94	57 479	133 478
2002 TQ65	15.36	2.81	0.10E-17	11.89	2.82	119.41	76 000	176 489
2002 TT67	16.09	2.01	0.17E-17	11.94	2.77	108.35	71 342	165 672
2002 TV68	17.99	0.84	0.57E-18	14.75	4.54	75.14	484 987	1 126 248
2002 TR96	15.99	2.11	0.16E-17	10.91	2.39	115.50	81 908	190 208
2002 TM190	14.16	4.89	0.12E-17	11.73	2.80	140.62	31 855	73 974
2002 UR12	16.10	2.00	0.17E-17	17.72	2.96	86.61	40 199	93 352
2002 UP36	17.13	1.25	0.26E-18	7.29	2.33	125.04	1 725 249	4 006 412
2002 VP94	17.14	1.24	0.35E-18	11.99	3.01	94.32	634 692	1 473 896
2002 YK29	17.98	0.84	0.14E-17	9.35	2.53	97.30	376 375	874 026
2003 BL	16.04	2.06	0.72E-18	18.20	3.68	85.98	89 383	207 568
2003 BM1 [13]	18.30	0.73	0.33E-18	8.08	2.47	101.35	2 375 798	5 517 132
2003 BA19	13.88	5.56	0.15E-17	12.76	2.84	139.07	20 064	46 593
2003 BU35	16.19	1.92	0.47E-18	10.86	3.32	112.83	307 978	715 193
2003 CC22	13.27	7.37	0.19E-19	9.44	2.77	178.43	1 644 499	3 818 892
2003 DA10	15.11	3.16	0.12E-17	11.89	3.09	123.35	58 049	134 803
2003 GB	15.41	2.75	0.93E-18	12.62	2.92	114.72	79 628	184 914
2003 JC11	18.74	0.59	0.91E-18	13.98	3.21	70.26	515 614	1 197 371
2003 KK20	17.78	0.92	0.18E-17	13.46	2.79	81.31	153 509	356 483
2003 SJ5	19.79	0.37	0.11E-17	13.29	3.10	63.08	875 317	2 032 680
2003 SC255	15.61	2.51	0.12E-17	11.66	2.79	116.88	80 468	186 863
2003 TA	18.14	0.78	0.12E-17	14.83	3.46	73.47	258 252	599 719
2003 UW	15.89	2.20	0.31E-19	7.23	2.37	147.58	7 107 220	16 504 543
2003 UR267 [14]	16.53	1.64	0.13E-18	7.54	1.95	132.63	2 341 997	5 438 638
2003 UY283	15.15	3.10	0.83E-21	12.37	0.00	120.00	78 441 720	182 159 104
2003 VA3	16.44	1.71	0.12E-17	11.70	2.71	104.73	130 577	303 228
2003 XX	16.55	1.63	0.18E-17	13.23	2.63	96.33	75 411	175 121
2003 YA	14.94	3.42	0.20E-17	11.02	2.57	131.63	34 568	80 275
2003 YH63	16.36	1.78	0.28E-18	13.95	3.98	95.83	406 654	944 341
2004 AE9	17.39	1.11	0.31E-18	11.11	2.67	95.31	940 805	2 184 758
2004 BT1 [15]	14.67	3.87	0.71E-19	9.02	2.61	152.63	1 074 427	2 495 058
2004 DO29	12.95	8.54	0.29E-18	12.41	3.87	159.41	60 167	139 722
2004 DA62	12.51	10.46	0.24E-18	18.13	3.16	136.29	33 506	77 808
2004 EU20	15.95	2.14	0.12E-17	13.92	2.85	101.19	75 468	175 253
2004 ET48	17.31	1.15	0.14E-17	11.39	2.68	94.97	192 328	446 628
2004 FN1	16.51	1.66	0.88E-18	13.78	2.94	94.63	143 986	334 367
2004 FC29	19.80	0.36	0.51E-18	14.42	3.15	60.16	1 640 783	3 810 262
2004 JD2	15.76	2.34	0.11E-17	12.10	2.76	112.25	86 339	200 499
2004 KZ7 [16]	15.32	2.87	0.72E-18	13.63	2.80	111.13	87 841	203 986
2004 LH18	19.54	0.41	0.95E-19	8.67	3.04	82.91	15 667 835	36 384 200
2004 MU7	14.86	3.54	0.75E-18	13.44	4.06	118.91	65 003	150 950
2004 PA44	13.53	6.54	0.28E-20	7.41	0.66	197.75	18 040 806	41 894 764
2004 RH9	17.04	1.30	0.84E-18	14.10	2.99	87.20	199 693	463 732
2004 RR109	17.42	1.09	0.78E-18	20.34	3.14	67.50	161 770	375 667
2004 RT109	18.45	0.68	0.26E-18	11.00	3.84	83.52	2 135 891	4 960 014
2004 RP111	17.87	0.89	0.45E-18	11.82	3.38	86.48	792 315	1 839 933
2004 RW141 [17]	14.29	4.61	0.60E-19	5.84	1.81	204.92	1 878 830	4 363 061

[13] $T_{\rm int}$ = 45 796 yr.
[14] $T_{\rm int}$ = 26 023 yr.
[15] $T_{\rm int}$ = 79 108 yr.
[16] $T_{\rm int}$ = 57 151 yr.
[17] $T_{\rm int}$ = 55126 yr.

Table 1. continued.

ACO	H	r_t km	$\langle P_i \rangle$ km^{-2} yr^{-1}	$\langle V_{col} \rangle$ km s^{-1}	$\sigma_{v_{col}}$	r_a	T_{200}	T_{100}
2004 RO288	16.45	1.70	0.82E-20	7.80	2.62	131.47	33 024 586	76 690 424
2004 SK	16.79	1.46	0.11E-17	13.41	3.24	92.66	143 921	334 216
2004 TS166	20.45	0.27	0.27E-17	9.52	2.50	69.88	835 583	1 940 409
2004 UZ	17.25	1.18	0.12E-17	10.76	2.59	98.83	223 665	519 401
2004 XL	17.12	1.25	0.80E-18	15.09	3.39	83.06	200 216	464 945
2004 XR17	16.15	1.96	0.10E-17	12.63	3.06	104.16	111 149	258 113
2004 XH50	16.53	1.64	0.72E-18	20.72	2.95	74.99	99 433	230 905
2004 XY100	15.25	2.96	0.15E-18	7.80	2.86	153.65	888 575	20 63 469
2004 XA131	13.25	7.44	0.86E-18	12.49	2.72	152.76	24 211	56 223
2004 YW	14.87	3.53	0.10E-17	12.51	2.87	123.66	52 564	122 064
2005 AY30	13.80	5.77	0.12E-17	12.81	2.79	140.21	231 52	53 763
2005 CR16	14.23	4.74	0.30E-18	11.11	3.82	143.69	146 213	339 540
2005 DE	17.32	1.14	0.10E-17	12.34	2.83	90.65	229 639	533 274
2005 EB127 [18]	15.78	2.32	0.92E-18	10.13	3.31	123.77	137 724	319 825
2005 GP81	15.84	2.26	0.22E-17	11.16	2.45	116.28	52 839	122 703
2005 JM3	19.90	0.35	0.89E-18	12.89	2.70	63.26	1 174 698	2 727 909
2005 JC46	16.67	1.54	0.76E-18	13.78	2.90	92.69	183 322	425 714
2005 JE173 [19]	15.99	2.11	0.34E-18	9.58	3.28	124.29	458 994	1 065 886
2005 KL8	16.36	1.78	0.11E-17	12.02	2.90	104.23	128 288	297 914
2005 NX43 [20]	16.44	1.71	0.92E-18	8.59	2.78	124.67	257 984	599 096
2005 NK61	16.47	1.69	0.60E-19	8.62	2.99	123.94	4 011 633	9 315 904
2005 QT176	17.73	0.94	0.10E-17	12.48	2.96	85.41	291 690	677 368
2005 RW9	16.68	1.53	0.11E-17	13.53	2.81	93.53	136 000	315 821
2005 SB216	12.33	11.36	0.35E-19	8.85	2.00	209.08	560 013	1 300 475
2005 TC53	16.75	1.48	0.79E-18	13.52	2.95	92.72	188 854	438 561
2005 VX116	13.14	7.82	0.17E-17	11.37	2.71	163.39	12 933	30 032
2005 WY3	13.51	6.60	0.26E-18	16.11	2.89	127.94	64 550	149 900
2005 WS54	18.23	0.75	0.76E-18	13.50	2.94	76.57	476 199	1 105 840
2005 XQ1	16.84	1.42	0.53E-18	15.92	3.41	83.57	237 755	552 119
2005 XK57 [21]	15.02	3.29	0.30E-18	12.09	2.43	123.63	207 738	482 413
2005 XV91	13.87	5.59	0.68E-19	9.75	2.78	162.07	630 605	1 464 404
2005 YW3	14.96	3.38	0.99E-18	12.34	2.75	123.17	59 232	137 551
2005 YW24 [22]	15.66	2.45	0.76E-19	8.97	2.60	134.64	1 840 053	4 273 012
2005 YQ127	15.15	3.10	0.40E-18	10.81	2.47	129.49	196 735	456 862
2005 YR204	16.68	1.53	0.12E-17	11.78	2.67	101.13	140 237	325 662
2006 BV7 [23]	19.58	0.40	0.29E-19	26.21	3.40	44.19	11 132 053	25 851 100
2006 BQ55	16.08	2.02	0.62E-18	16.00	3.20	91.98	126 997	294 916
2006 BF208	14.40	4.38	0.52E-18	13.95	2.72	123.61	67 727	157 277
2006 BH257	13.51	6.60	0.18E-18	8.14	3.16	188.03	252 892	587 271
2006 DQ153	16.28	1.84	0.11E-17	11.90	2.75	105.91	124 055	288 084
2006 EA1	19.57	0.40	0.18E-17	11.89	2.53	69.11	528 780	1 227 944
2006 ED1	18.58	0.64	0.71E-18	15.02	3.06	68.89	544 388	1 264 190
2006 ES36	17.94	0.86	0.11E-17	13.59	3.16	79.21	277 825	645 171
2006 FV4	12.90	8.74	0.13E-18	11.65	2.56	166.27	146 705	340 681
2006 FH51	18.07	0.81	0.13E-17	12.39	2.80	82.05	290 534	674 685
2006 HS [24]	15.18	3.06	0.40E-18	17.76	4.04	97.48	99 074	230 071

[18] T_{int} = 17 774 yr.

[19] T_{int} = 75 332 yr.

[20] T_{int} = 28 392 yr.

[21] T_{int} = 49 969 yr.

[22] T_{int} = 50 370 yr.

[23] T_{int} = 12 766 yr.

[24] T_{int} = 24 073 yr.

Table 1. continued.

ACO	H	r_{t} km	$\langle P_{\mathrm{i}} \rangle$ km^{-2} yr^{-1}	$\langle V_{\mathrm{col}} \rangle$ km s^{-1}	$\sigma_{v_{\mathrm{col}}}$	r_a	T_{200}	T_{100}
2006 HP131 [25]	18.11	0.79	0.95E-18	8.06	2.13	104.03	739 433	1 717 128
2006 HT131	17.33	1.14	0.17E-17	8.50	2.64	111.72	244 219	567 131
2006 JO65 [26]	17.03	1.30	0.48E-18	8.45	3.21	116.55	712 295	1 654 107
2006 QL39	13.58	6.39	0.23E-19	9.99	1.75	166.00	1 484 856	3 448 167
2006 RN16	13.90	5.51	0.45E-19	7.01	2.55	194.47	1 547 351	3 593 293
2006 SO134 [27]	16.43	1.72	0.38E-19	8.28	1.39	127.45	6 426 652	14 924 113
2006 SH281	14.23	4.74	0.19E-17	10.62	2.59	147.39	24 573	57 064
2006 SV301	14.30	4.59	0.13E-18	8.05	2.36	170.76	543 258	1 261 567
2006 TP	16.80	1.45	0.12E-17	11.47	2.79	101.07	168 601	391 529
2006 UE63	19.80	0.36	0.24E-18	10.58	2.61	71.64	5 539 549	12 864 065
2006 UJ170	18.14	0.78	0.11E-17	13.11	3.11	78.76	315 397	732 421
2006 WR3	15.64	2.47	0.66E-18	17.16	3.45	93.62	83 630	194 208
2006 WS3	16.97	1.34	0.22E-18	13.81	3.52	89.03	760 855	1 766 875
2006 WF6	16.47	1.69	0.72E-18	8.95	2.66	121.34	315 861	733 498
2006 XL5	16.79	1.46	0.19E-18	8.06	2.49	123.49	1 691 704	39 28 513
2006 YC	14.07	5.10	0.20E-17	18.18	2.95	111.12	10 024	23 279
2007 AD12	15.75	2.35	0.13E-17	9.65	2.87	127.70	99 807	231 774
2007 AK22	15.88	2.22	0.15E-17	9.85	2.42	124.12	91 869	213 341
2007 BU3	15.39	2.78	0.13E-17	12.03	2.58	118.16	61 073	141 826

[25] T_{int} = 5480 yr.
[26] T_{int} = 56 236 yr.
[27] T_{int} = 10 191 yr.